Thin–Walled Structures 205 (2024) 112367

Contents lists available at ScienceDirect

Thin-Walled Structures

journal homepage: www.elsevier.com/locate/tws

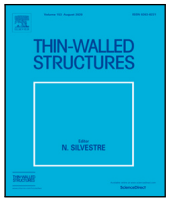

Full length article

Probabilistic resistance predictions of laterally restrained cellular steel beams by natural gradient boosting

Vitaliy V. Degtyarev [a], Stephen J. Hicks [b], Felipe Piana Vendramell Ferreira [c], Konstantinos Daniel Tsavdaridis [d,*]

[a] New Millennium Building Systems, LLC, 3700 Forest Dr. Suite 501, Columbia, SC 29204, United States of America
[b] School of Engineering, University of Warwick, Coventry, CV4 7AL, United Kingdom
[c] Faculty of Civil Engineering – Campus Santa Mônica, Uberlândia, Federal University of Uberlândia, Minas Gerais, Brazil
[d] Department of Engineering, School of Science and Technology, City, University of London, Northampton Square, London EC1V 0HB, United Kingdom

ARTICLE INFO

Dataset link: https://data.mendeley.com/datasets/zcm29bp7yf/1, https://scbra.herokuapp.com/

Keywords:
Cellular beams
Lateral restraint
Machine learning
Natural gradient boosting
Resistance
Reliability

ABSTRACT

Accurate and reliable cellular steel beam resistance predictions are essential for economical and safe designs of steel-framed buildings with such beams. This paper proposes a new machine-learning (ML) model based on the natural gradient boosting (NGBoost) algorithm to predict probabilistic load-bearing capacities of laterally restrained cellular beams subjected to uniformly distributed loads, considering all possible failure modes and their interactions. The NGBoost model was developed based on a database with 14,094 numerical simulation results and interpreted using the SHapley Additive exPlanations (SHAP) method commonly used for ML model explanation and interpretation. The resistance reduction factors required for the NGBoost model to meet the reliability requirements of the European and US design frameworks were determined via reliability analyses using the methods given in the respective standards and the improved Hasofer–Lind–Rackwitz–Fiessler (iHL-RF) method. Comparisons of the developed NGBoost model with other ML models and existing design provisions indicate that the former is as accurate as other ML models (while offering probabilistic predictions) and significantly outperforms the existing design provisions. A web application was developed and deployed online to predict the ultimate uniform loads of laterally restrained cellular beams with the developed NGBoost model. The proposed NGBoost model can facilitate preliminary cellular steel beam designs and investigating parameters affecting their resistance.

1. Introduction

Cellular steel beams, distinguished by regularly spaced circular web openings, have gained popularity in construction due to their lightweight and ability to span long distances and integrate services within the structural floor depth [1,2]. However, the structural design of such beams is more complex compared with solid-web beams due to the need to analyze multiple failure modes, such as lateral–torsional buckling (LTB), beam global shear (BGS), beam global bending (BGB), Vierendeel bending of the Tees (VBT), web-post shear (WPS), and web-post buckling (WPB) [1,2].

Many studies investigated the resistance of cellular steel beams experimentally [3–11] and numerically [5,8–10,12–20]. Based on the results of the experimental and numerical studies, several design provisions have been developed over the years, including SCI P100 [21], ENV 1993-1-1: 1992/A2: 1998 [22], SCI P355 [1], FprEN 1993-1-13 [23], and AISC Design Guide 31 (AISC DG31) [2]. However, capturing all failure modes by simple empirical formulae that are suitable for design guides and standards has been found to be challenging due to the problem complexity. As a result of this, the existing design provisions do not always predict the resistance of cellular steel beams accurately [24–26] (by largely underestimating them), which highlights opportunities for design model improvements.

Machine learning (ML), which has been successfully used in many structural engineering applications [27–29], can offer design models for cellular steel beams that are more accurate than those given within existing design provisions. Over the recent years, several publications presented ML models for predicting the resistance of cellular beams [30–36], castellated beams [37], and beams with elliptical [38,39], and sinusoidal [40] web openings. Some published ML models produced beam resistances against a single failure mode, such as LTB [30,

* Corresponding author.
E-mail addresses: vitaliy.degtyarev@newmill.com (V.V. Degtyarev), stephen.j.hicks@warwick.ac.uk (S.J. Hicks), fpvferreira@ufu.br (F.P.V. Ferreira), konstantinos.tsavdaridis@city.ac.uk (K.D. Tsavdaridis).

https://doi.org/10.1016/j.tws.2024.112367
Received 13 May 2024; Received in revised form 5 August 2024; Accepted 22 August 2024
Available online 28 August 2024

34,36,40], WPB [33,38,39], and lateral–distortional buckling [37], while others predicted elastic buckling loads [31,32,35] or the beam resistance covering all possible failure modes [35]. The published ML models were based on various algorithms, with artificial neural network (ANN) being the most popular [30,31,33,34,37–40]. The ML models described in [35] relied on decision tree (DT), random forest (RF), k-nearest neighbor (KNN), gradient boosting regressor (GBR), extreme gradient boosting (XGBoost), light gradient boosting machine (LightGBM), and gradient boosting with categorical features support (CatBoost). Ly et al. [32] employed adaptive neuro-fuzzy inference system (ANFIS), while Seghier et al. [36] developed their models based on least square support vector machine (LSSVM).

All published ML models for predicting the resistance of cellular steel beams applied to one failure mode, laterally unrestrained beams, or beams with a lateral restraint provided at mid-span because they were trained on such data. As a result, the existing ML models covering all possible failure modes are limited by relatively short spans, further increase of which is impossible without provision of lateral restraints to eliminate the LTB failure mode. For example, the ML models presented in [35] applied to the beams with a maximum span of 7 m, or from $10.0H$ for 700-mm deep beams to $16.7H$ for 420-mm deep beams, where H is the beam height. In construction, transversely orientated steel decking restrains cellular beams laterally when it is appropriately attached to the beam compression flange [2,41]. Laterally restrained beams possess longer spanning capabilities than unrestrained beams as LTB is not a critical failure mode. This is reflected in beam spans typically in excess of 12.0 m [42]. As a result, long-span laterally restrained cellular beams provide a higher potential for possible interactions of different failure modes due to the internal force redistribution compared to short-span beams, thereby affecting the beam resistance. All available publications describe ML models for predicting the deterministic beam resistances, with no reliability-based calibrations of the models, which are considered necessary to ensure that the models produce resistances meeting the reliability requirements of respective building codes.

To address the above issues, this paper proposes an ML model for predicting probabilistic ultimate uniform loads of laterally restrained cellular steel beams spanning from $15H$ to $30H$, commonly used in steel-framed construction, especially for multi-storey commercial developments. The model is based on an extensive database with 14,094 finite element (FE) simulation results and the natural gradient boosting (NGBoost) algorithm [43], which was previously used in structural engineering applications [44–50] but not for cellular beams. NGBoost produces probabilistic outputs (herein beam resistances) that are unavailable from other ML models previously employed for cellular steel beams. The proposed NGBoost model for predicting cellular beam resistances was calibrated via reliability analyses for the Eurocode (EC) and US design frameworks, which also makes this study novel.

The paper has the following structure. Section 3 describes the database used for the NGBoost model training and evaluation. Section 4 overviews the NGBoost algorithm, describes the developed NGBoost model, and presents the results of the model interpretation. Section 5 presents the reliability-based calibration of the NGBoost model. Section 6 compares the NGBoost model predictions with those by ML models based on other ML algorithms and existing design provisions. A web application featuring the developed NGBoost model is described in Section 7.

2. Data acquisition

The data for training and evaluating the presented NGBoost model were obtained from a numerical parametric study that involved geometrically and materially nonlinear FE method analyses with imperfections (GMNIA). Similar approaches with ML models trained using numerical data obtained from FE simulations on validated models have been employed by many researchers for steel beams with regularly spaced web openings [31–40].

This section briefly describes the FE models of the cellular steel beams with geometric parameters illustrated in Fig. 1 and their validation. The scope of the numerical study is covered by the variable ranges described in Section 3.

2.1. FE models

The FE analyses were performed in ANSYS on cellular beam models created using quadrilateral shell elements SHELL181, with a maximum size of 20 mm, which was reduced by a factor of two in the vicinity of the openings. The mesh size that provided both the highest accuracy and computational efficiency was determined from a convergence study.

The elastic-perfectly plastic stress–strain diagram with an elastic modulus of 200 GPa and Poisson's ratio of 0.3 were assumed for the steel. Steel plasticity was modeled with isotropic hardening and von Mises yield criterion.

The model boundary conditions simulated a simply-supported beam, with symmetric boundary conditions applied at mid-span. The beam top (compression) flanges were laterally restrained at a spacing ranging from 300 to 348 mm, simulating steel deck attachments. Uniformly distributed loads were applied to the beam top flange nodes at the web location with vertical forces, the magnitude of which was proportional to the corresponding FE size. Full-height web stiffeners with a thickness equal to the beam flange thickness were provided at the beam supports. Fig. 2 shows a typical FE model of a cellular steel beam used in the study.

The initial geometric imperfections, with a magnitude of $H/100$ for $L/H < 10$ and $L/1000$ for $L/H \geq 10$ [7,18,20], were assumed to match the beam's first buckling mode obtained from the elastic buckling analysis, which preceded the nonlinear analysis.

The residual stresses with the following magnitudes [7,16,51] were applied to the models. Compressive stresses at the flange edges were 100 MPa for $(H + t_f)/b_f > 1.2$ and 150 MPa for $(H + t_f)/b_f \leq 1.2$. Tensile stresses at the flange center were 50 MPa for $(H + t_f)/b_f > 1.2$ and 100 MPa for $(H + t_f)/b_f \leq 1.2$. Tensile stresses in the web were $50 b_f t_f/[(H - h_o)t_w]$.

Large-deflection effects (geometric nonlinearity) were allowed in the static analyses in addition to the material nonlinearity. The ultimate uniform loads were obtained by considering criteria C1 and C2 of prEN 1993-1-14 [52], which correspond to the maximum load the model could support and the largest tolerable strain, respectively. The largest tolerable total strains of 21%, 20%, and 17% were assumed for steel with the yield strengths of 275, 355, and 460 MPa, respectively, in accordance with EN 10 025-2 [53].

The ultimate uniform load obtained from the FE simulations for each beam was treated as the beam resistance; namely, the ability of the beam to withstand the external uniform load before it fails. In traditional cellular beam design, beam resistances for different limit states, such as bending resistance, shear resistance, web buckling resistance, etc., are usually computed and compared with the internal beam forces due to the applied external loads. The maximum permissible external load can be determined from the governing resistance using engineering mechanics principles, producing the beam resistance in terms of the applied load. In this paper, the term resistance, mainly used to shorten the text, refers to the ultimate uniform load.

2.2. Validation of the FE models

Ten physical test results presented in [3–5,9] were used for FE model validation. The tests were selected to represent the parametric study variables as closely as possible and cover multiple failure modes typical for cellular beams. The parameters of the selected beams and

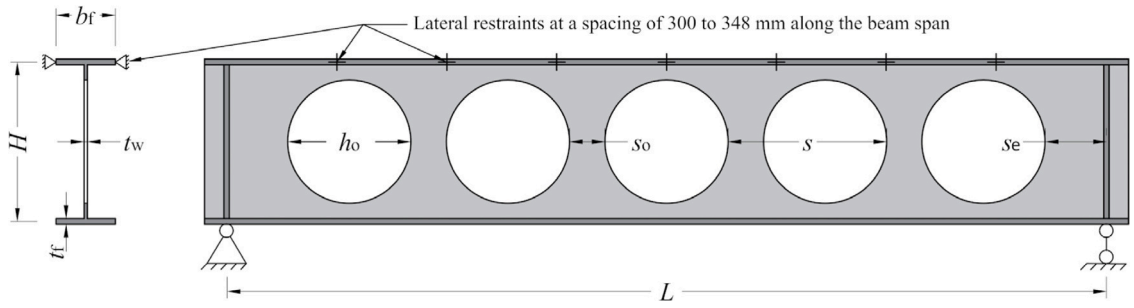

Fig. 1. Geometric parameters of cellular steel beams.

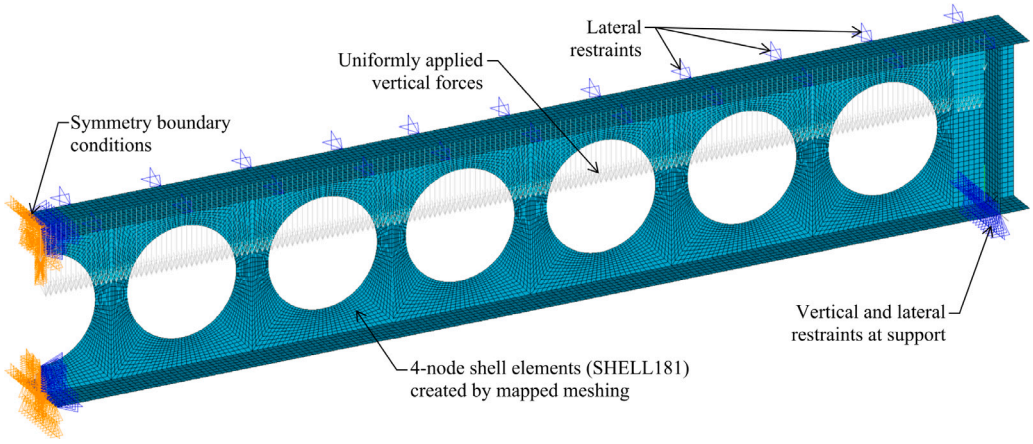

Fig. 2. FE model of a cellular steel beam.

Table 1
FE model validation results.

No.	Source	Test	L/H	H/h_o	s/h_o	f_y (MPa)	FM	P_{test} (kN)	P_{FEA} (kN)	P_{test}/P_{FEA}
1	[3]	1B	20	1.41	1.50	323	VBT	108.0	109.5	0.99
2	[3]	2B	19	1.34	1.33	343	VBT	117.0	119.6	0.98
3	[3]	3A	9	1.43	1.50	350	VBT	151.0	151.4	1.00
4	[3]	4A	18	1.40	1.23	437	BGB	90.0	90.0	1.00
5	[3]	4B	16	1.40	1.23	360	WPB	114.0	118.2	0.96
6	[5]	A1	4	1.39	1.30	360	WPB	288.7	286.8	1.01
7	[5]	B1	4	1.39	1.20	360	WPB	255.0	247.0	1.03
8	[4]	1-ss	3	1.52	1.34	338	WPB	500.0	490.9	1.02
9	[9]	A1	4	1.23	1.14	415	WPB	76.0	78.8	0.96
10	[9]	B6	4	1.63	1.40	390	WPB	299.9	304.2	0.99

Notes: FM = Failure mode; BGB = Beam global bending; VBT = Vierendeel bending of the Tees; WPB = Web-post buckling.

FE model validation results are summarized in Table 1. Comparisons of the load–displacement curves are shown in Fig. 3.

The information presented in Table 1 and Fig. 3 indicates a good prediction accuracy of the FE models characterized by the P_{test}/P_{FEA} values ranging from 0.96 to 1.03, with a mean value of 0.99 and a coefficient of variation (CoV) of 0.022.

The numerical study aimed to investigate the resistance of steel cellular beams with relatively large dimensions typical of those found in real steel-framed buildings, whereas test results for smaller beams have been reported in the literature because testing long-span beams at full-scale is expensive and not always feasible. As a result, the dimensions of the beams used for the FE model validation were smaller than those for the beams considered in the parametric study, but the relative dimensions, including L/H, H/h_o, s/h_o, and the yield strength of the tested and simulated beams were comparable. It should also be noted that the authors are unaware of published test results for cellular beams subjected to uniformly distributed loads. Therefore, the tests of the beams under concentrated loads were used for the FE model validation.

The tested beams failed in three failure modes, including BGB, VBT, and WPB (see Table 1). The model validation did not include the BGS and WPS failure modes because the authors are unaware of test results for these failure modes suitable for FE model validation. The LTB failure mode was not considered, because the studied beams were laterally restrained, which prevented this failure mode.

It can be concluded that the developed FE models could accurately predict the resistance and behavior of cellular steel beams with different dimensions and mechanical properties failing in various failure modes. Therefore, the FE models were found appropriate for the numerical parametric study.

2.3. Failure modes observed in the numerical study

The simulated beams demonstrated various failure modes and their interactions, as can be seen from the images of von Mises stress contours at the beam failures presented in the database [54]. The authors believe the multiple interactions of the failure modes were facilitated by the LTB failure mode prevention, which allowed for the internal force redistribution within long-span beams.

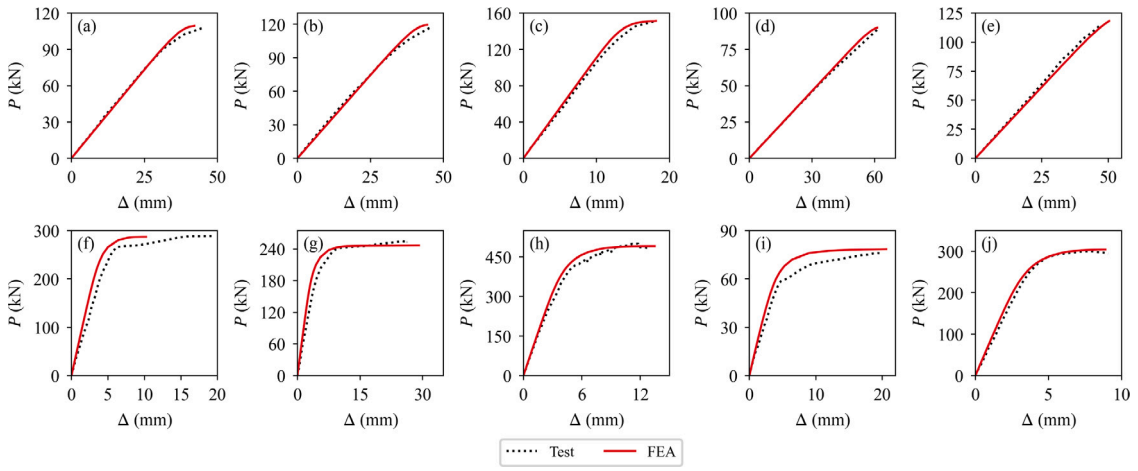

Fig. 3. Comparisons of the load–displacement curves from the tests and FE simulations (a) 1B [3], (b) 2B [3], 3 A [3], 4 A [3], 4B [3], A1 [5], B1 [5], 1ss [4], A1 [9], and B6 [9].

Table 2
Statistical parameters of the database variables.

Variables	Min.	Max.	Mean	St. Dev.	Skewness	Kurtosis
H (mm)	420.0	700.0	560.0	114.3	0.00	−1.50
b_f (mm)	162.0	270.0	216.0	44.1	0.00	−1.50
t_w (mm)	9.0	15.0	12.0	2.4	0.00	−1.50
t_f (mm)	15.0	25.0	20.0	4.1	0.00	−1.50
L/H	15.0	30.0	22.9	5.4	−0.10	−1.27
L (m)	6.30	21.00	12.84	4.06	0.40	−0.64
H/h_o	1.25	1.70	1.48	0.19	−0.12	−1.55
s/h_o	1.10	1.49	1.29	0.16	0.06	−1.58
h_o (mm)	247.1	560.0	383.9	93.4	0.34	−0.75
s (mm)	271.8	834.4	495.4	137.0	0.53	−0.25
s_o (mm)	24.7	274.4	111.4	70.3	0.54	−0.70
s_e (mm)	25.2	960.4	264.6	182.5	1.11	1.14
f_y (MPa)	275.0	460.0	363.3	75.8	0.16	−1.50
n_o	11.0	46.0	26.0	8.2	0.31	−0.52
P	1.00	2.00	1.38	0.49	0.50	−1.75
w_u (kN/m)	6.85	249.96	44.87	31.98	1.64	3.28

The NGBoost model presented in this study predicts the resistance of cellular beams failing in all possible failure modes and their interactions, while it does not identify the governing failure mode, which is similar to the ML models presented in [35].

3. Database

The NGBoost model described in this paper was developed using a database of uniformly distributed ultimate loads, w_u, applied to simply-supported laterally restrained cellular steel beams [54]. The database includes 14,094 FE simulation results for the beams with various depths, H, web thicknesses, t_w, flange widths, b_f, and thicknesses, t_f, span-to-depth ratios, L/H, depth-to-opening diameter ratios, H/h_o, opening spacing-to-diameter ratios, s/h_o, and yield strengths, f_y.

Table 2 presents the statistical parameters of the database variables, with n_o being the number of web openings in each beam and P corresponds to the distribution of n_o taken as 1 and 2 for the odd and even numbers of the openings, respectively. Fig. 4 shows distributions of the database features. Table 2 and Fig. 4 indicate that the database covers a wide range of cellular steel beams commonly found in modern construction.

The correlation matrix in Fig. 5 presents the Pearson correlation coefficients for the database variables. It indicates that the independent database variables practically do not correlate with each other (except for H and L showing a moderate correlation), making the independent variables appropriate candidates for the NGBoost model features. Fig. 5 also indicates that L and s/h_o are moderately correlated with w_u (negatively and positively, respectively), while other independent variables are weakly correlated with w_u.

4. Natural gradient boosting NGBoost model

4.1. Overview of the NGBoost algorithm

Natural gradient boosting (NGBoost), introduced by Duan et al. [43], is a supervised learning technique designed to enable probabilistic predictions through the utilization of gradient boosting [55] and natural gradient algorithms [56].

The traditional regression boosting algorithms, such as XGBoost [57], LightGBM [58], and CatBoost [59] produce a deterministic scalar prediction for each set of features, treated as the mean prediction. In contrast, NGBoost produces the mean and standard deviation for each feature set. These two parameters and the distribution type, specified before model training, describe a full probability distribution for each prediction. NGBoost employs a scoring rule, such as the logarithmic or continuous ranked probability score, that compares the predicted probability distribution with the observed data to allow for probabilistic predictions. Using a scoring rule instead of a loss function differentiates NGBoost from the traditional boosting algorithms. For a comprehensive description of the NGBoost algorithm, readers are referred to [43].

NGBoost requires several hyperparameters to be specified before model training, including those related to the base learner (decision tree), gradient boosting, and natural gradient.

4.2. Proposed NGBoost model

The NGBoost model for predicting the ultimate uniform loads of laterally restrained cellular steel beams was developed using an open-source Python library *ngboost* (https://github.com/stanfordmlgroup/ngboost). The model features included H, b_f, t_w, t_f, L, H/h_o, s/h_o, f_y, and P. These nine features were selected based on an exploratory study where different feature sets were tested. The selected features align well with the empirical and mechanics-based knowledge of the parameters affecting the cellular beam resistance. The features were not strongly correlated between themselves (see Fig. 5, confirming the appropriate feature selection).

Scikit-learn's [60] ten-fold cross-validation was employed to validate the model, with 80% and 20% of the data assigned to training and test sets, respectively. Feature values were standardized before model training to facilitate convergence of the NGBoost algorithm. The root-mean-square error (RMSE= $\sqrt{(1/n)\sum_{i=1}^{n}(y-x)^2}$, where n is

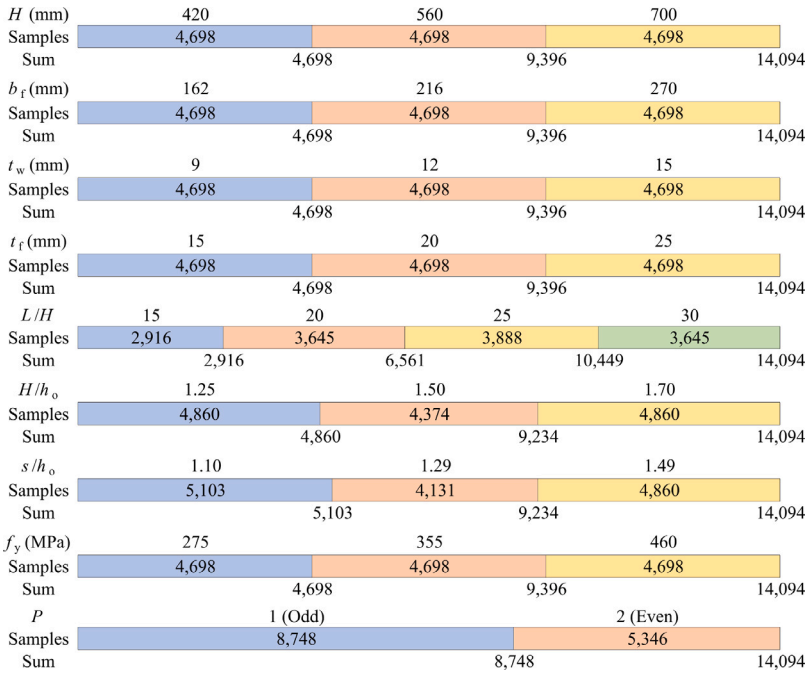

Fig. 4. Distributions of database features.

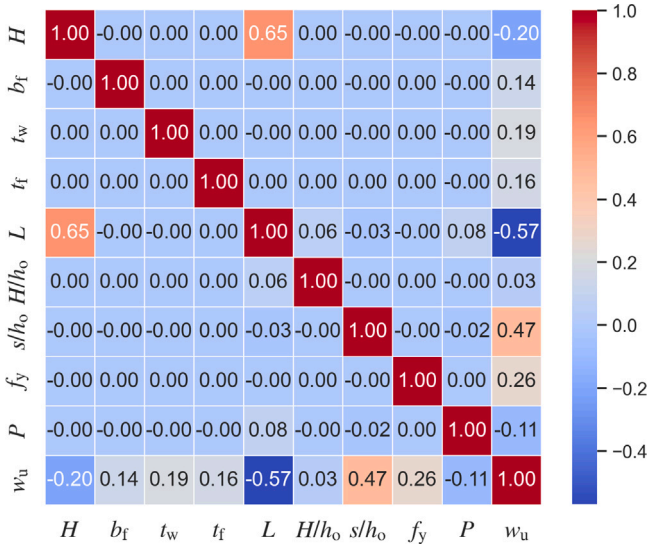

Fig. 5. Correlation matrix.

the number of observations, y is the observed values, and x is the predicted values) and the coefficient of determination ($R^2 = 1 - \sum_{i=1}^{n}(y-x)^2 / \sum_{i=1}^{n}(y-\bar{y})^2$, where $\bar{y}$ is the mean value of y) were used for assessing the NGBoost model performance. The latter error metric (R^2) is considered by some researchers more informative than other error metrics commonly used for model performance evaluation [61].

The NGBoost model hyperparameters were optimized in *Optuna* [62], a Python library for automatic hyperparameter optimization featuring *define-by-run* programming, efficient sampling and pruning algorithms, and easy-to-setup versatile architecture. Table 3 summarizes hyperparameter optimization results. The lognormal distribution, which was found to be more appropriate than the normal distribution, was specified as a model hyperparameter, as well as the logarithmic score.

Fig. 6 shows the optimal NGBoost model performance in predicting mean values of the ultimate uniform load, which can be treated as

Table 3
Hyperparameter optimization results.

Hyperparameter	Search range	Optimal value
Max_depth	3 to 20	7
Min_samples_split	2 to 50	10
Min_samples_leaf	2 to 50	5
Max_features	2 to 9	6
n_estimators	100 to 3000	2500
Learning_rate	0.01 to 0.20	0.05

the nominal beam resistance. RR in Fig. 6 stands for the resistance ratio, which is the ratio of the FE simulation results to the NGBoost model predictions. CoV is the coefficient of variation. Fig. 6 indicates an exceptional prediction accuracy of the developed model, with no overfitting seen from the model performance comparison for the train and test sets.

Table 4 gives performance metrics for the NGBoost model for various subsets corresponding to different European steel grades considered in the study. Table 4 indicates that the model performance worsens slightly when the steel grade increases based on the RMSE values. However, the differences in the other performance metrics are relatively small and practically imperceptible.

Fig. 7 presents RRs for the NGBoost model as functions of the model features. These graphs allow for visual evaluations of the model performance along the entire range of the feature values. The zero-slopes of the linear regression lines in Fig. 7 (shown in red) and relatively low scatters of the data points indicate accurate predictions within the model applicability limits, which correspond to the feature ranges in the database [54] used for model training (see Table 2).

Probabilistic predictions of the NGBoost model for three selected data samples representing the minimum, mean, and maximum RR values are shown in Fig. 8, with the sample numbers corresponding to those in the database [54]. For comparison purposes, Fig. 8 also shows the w_u values from the FE simulations and those predicted by the existing design provisions, including SCI P355 [1], FprEN 1993-1-13 [23] (with both the main and alternative VBT provisions), and AISC DG31 [2].

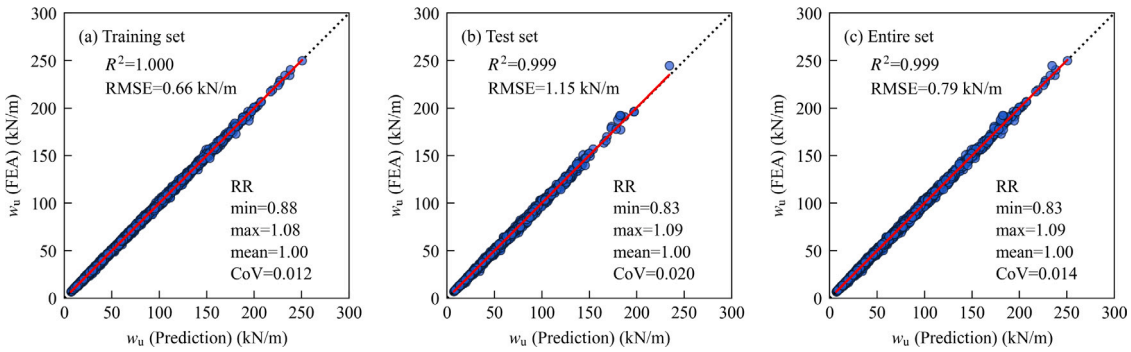

Fig. 6. Performance of the NGBoost model in predicting the mean beam resistance.

Table 4
NGBoost model performance (mean resistance).

Steel grade	RMSE (kN/m)			R^2			RR mean			RR CoV		
	Train	Test	All	Train	Test	All	Train	Test	All	Train	Test	All
S275, S355, S460	0.66	1.15	0.79	1.000	0.999	0.999	1.000	1.000	1.000	0.012	0.020	0.014
S275	0.43	1.15	0.64	1.000	0.997	0.999	1.000	0.999	1.000	0.009	0.025	0.014
S355	0.55	1.42	0.80	1.000	0.998	0.999	1.000	0.999	1.000	0.010	0.024	0.014
S460	0.71	1.90	1.06	1.000	0.997	0.999	1.000	1.000	1.000	0.010	0.026	0.014

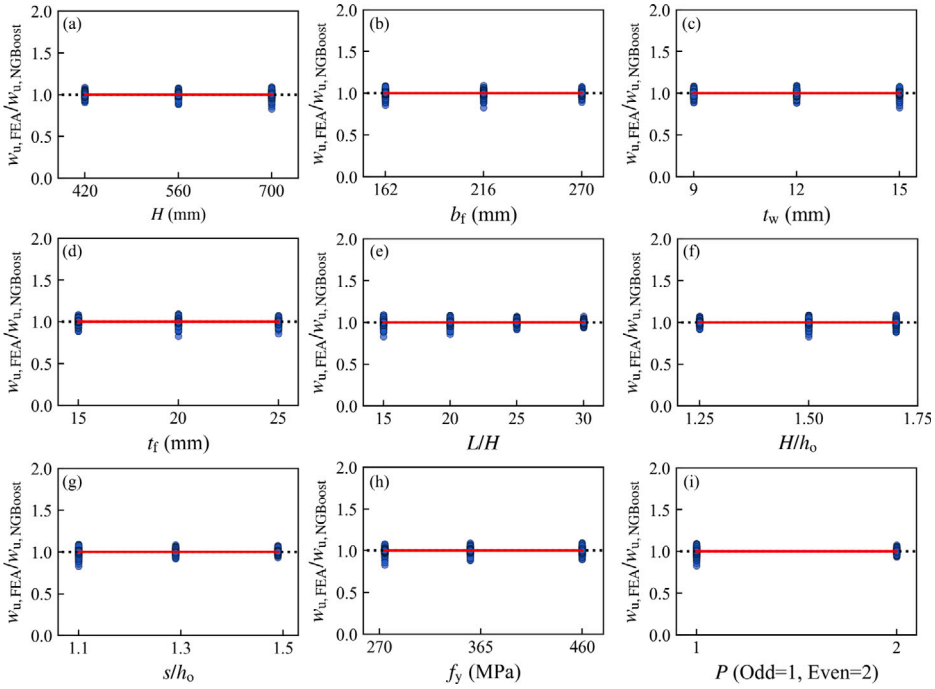

Fig. 7. Simulation-to-prediction ratios versus database variables.

4.3. NGBoost model interpretation

The developed NGBoost model was interpreted using the SHapley Additive exPlanations (SHAP) method [63] to provide insights on how and why the model makes predictions. The SHAP method, which has been widely used for interpreting models based on various ML algorithms, relies on the cooperative game theory [64] to estimate the contribution of each feature to the model output by considering Shapley values estimated from comparing model predictions with and without each feature.

Fig. 9 shows a SHAP summary plot, which ranks the features based on their effects on the model predictions. The colors ranging from red to blue represent each feature's value varying from high to low, respectively. Fig. 9 indicates that the beam span length, L, and the relative opening spacing, s/h_o, have the most significant effects on the ultimate uniform load, w_u, predicted by the model. Longer span beams and smaller opening spacings correspond to lower beam resistances. The steel yield strength, f_y; web thickness, t_w; beam height, H; flange thickness, t_f; flange width, b_f, and the H/h_o ratio have less significant impacts on model output than L and s/h_o.

Fig. 9 also shows that the predicted w_u values increase when f_y, t_w, H, t_f, b_f, and H/h_o increase, which aligns with the mechanics-based knowledge. The parity of the number of openings affects the NGBoost model predictions the least, with lower w_u values corresponding to the beams with an even number of openings, which relates to the web-post and opening locations relative to the internal beam forces due to the applied load. In other words, the web-posts and opening centers of the beams with an even number of openings were located in zones

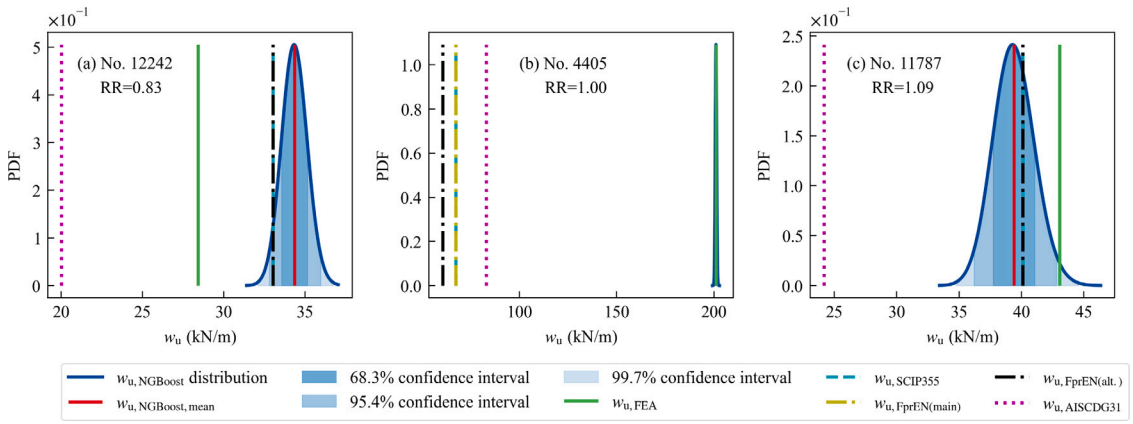

Fig. 8. Probabilistic predictions of the nominal beam resistance by the NGBoost model for individual beams.

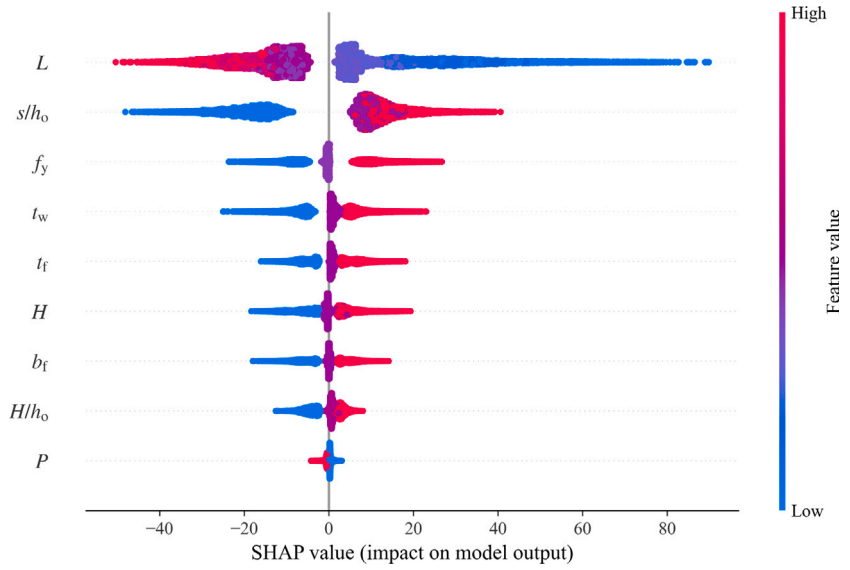

Fig. 9. SHAP summary plot for the NGBoost model.

with higher internal forces than those of beams with an odd number of openings.

Fig. 10 presents SHAP dependence plots, illustrating how changes in each feature value affect model predictions, considering all possible failure modes covered by the model. The colors in the graphs correspond to the second feature, shown in the secondary vertical axis, which has the most significant interaction with the analyzed feature.

Figs. 10(a) and (c) indicate that w_u increases when H and t_w increase, with more significance to shorter beam spans. The effect of t_w on w_u can be explained by the higher susceptibility of short-span beams to web-post buckling and shear failure modes, the resistances against which are highly dependent on the web thickness.

According to Figs. 10(b), (d), (f), and (h), w_u increases when b_f, t_f, H/h_o, and f_y increase, with the more significant increase in the beam resistance corresponding to higher s/h_o values. This can be explained by the fact that b_f, t_f, H/h_o, and f_y affect the Vierendeel bending resistance of the Tees (VBT) more significantly than the beam resistance against other failure modes. The VBT failure mode is more likely to govern the beam resistance when the opening spacing is relatively wide, which is consistent with that reported within the literature. When s/h_o is small, the web-post buckling and shear, which are practically unaffected by b_f, t_f, and H/h_o, govern the beam resistance in many cases.

Fig. 10(e) indicates that w_u reduced nonlinearly when L increased, with greater declines in w_u corresponding to L changing from 6.3 to 12.6 m and smaller w_u reductions when L increased from 12.6 to 21.0 m. More significant w_u decreases due to an L increase were associated with wider web opening spacings (see the red points in Fig. 10(e)), which is explained as follows: for small s/h_o values, WPS and WPB failure modes would likely govern the beam resistance; these failure modes are affected by L less significantly than others.

Fig. 10(g) shows a relatively steep increase in w_u when s/h_o increased from 1.10 to 1.29 and a smaller w_u increase for s/h_o changing from 1.29 to 1.49. Larger w_u increases are associated with shorter beam spans, for which increasing the opening spacing resulted in primary failure modes changes from WPS or WPB to others with higher resistances. For longer spans, widening the opening spacing may also result in changing the governing failure mode, but the resistances against BGS, BGB, and VBT are lower than those for shorter spans, resulting in smaller w_u increases.

According to Fig. 10(i), w_u reduces slightly when the web openings along the beam span changes from an odd ($P = 1$) to an even number ($P = 2$), with a more significant decrease associated with shorter beam spans when compared with longer spans. The reduction can be explained by shifting the openings and web-posts to the locations with higher internal moments and shear forces when the opening number changes from odd to even and a higher sensitivity of short-span beams to opening location changes compared to long-span beams.

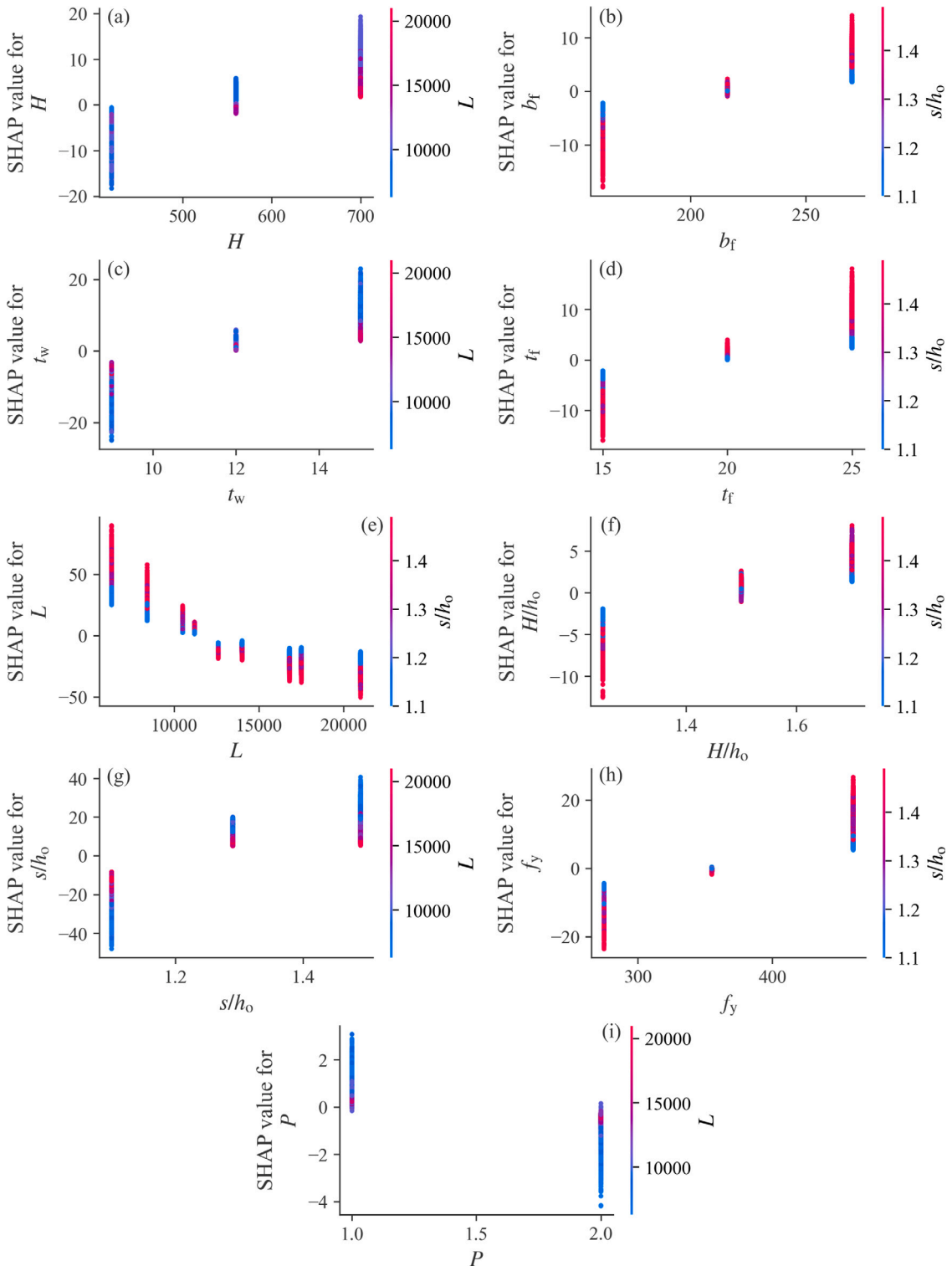

Fig. 10. SHAP dependence plots.

Overall, the NGBoost model interpretation results presented in this section align well with the empirical- and mechanics-based knowledge, indicating that the model can capture important mechanical relationships occurring in cellular beams under loads from the data.

5. Reliability-based calibrations of the NGBoost model

The NGBoost model described in Section 4 predicts nominal resistances of laterally restrained cellular beams. The model must be calibrated to ensure that its design predictions satisfy the reliability requirements of building codes.

This section presents reliability-based calibrations of the NGBoost model in accordance with the Eurocode (EC) and US design frameworks using the following two approaches: (1) calculating appropriate reduction factors with simplified methods presented in appropriate standards and (2) computing reliability indices, β, using the improved Hasofer–Lind–Rackwitz–Fiessler (iHL-RF) method [65–67] for different live-to-dead load ratios, with subsequent determination of required

Table 5
Statistical properties of random variables.

Properties	Variables	Mean (bias)	CoV	Distribution	Reference
Geometry	H/H_n	1.00	0.009	Lognormal	[41]
	b_f/b_{fn}	1.00	0.009	Lognormal	[41]
	t_w/t_{wn}	1.00	0.025	Lognormal	[41]
	t_f/t_{fn}	0.98	0.025	Lognormal	[41]
	L/L_n	1.00	0.001	Lognormal	[74]
	h_o/h_{on}	1.01	0.006	Lognormal	[74]
	s/s_n	1.00	0.008	Lognormal	[74]
Material	f_y/f_{yn} for f_{yn} = 275 MPa	1.25	0.055	Lognormal	[41]
	f_y/f_{yn} for f_{yn} = 355 MPa	1.20	0.050	Lognormal	[41]
	f_y/f_{yn} for f_{yn} = 460 MPa	1.15	0.045	Lognormal	[41]
	E_s/E_{sn}	1.00	0.030	Lognormal	[41]
Load	D/D_n (US)	1.05	0.100	Normal	[75]
	D/D_n (Europe)	1.00	0.100	Normal	[76]
	L/L_n (US)	1.00	0.250	Gumbel	[75]
	L/L_n (Europe)	0.60	0.350	Gumbel	[76]
Model error	ME	Table 4	Table 4	Lognormal	This study

reduction factors from comparisons of the obtained reliability indices with their target values specified within standards.

In the first approach, the partial factors required for the NGBoost model were calculated in accordance with Annex D of EN 1990 [68] for the EC framework, while the required load and resistance factor design (LRFD) resistance factors and allowable strength design (ASD) safety factors were determined in accordance with the AISI S100 [69] Chapter K requirements, modified to apply to cellular hot-rolled steel beams analyzed in the study. In a similar way to previous studies [70–73], the EN 1990 [68] Annex D and AISI S100 [69] Chapter K reliability analyses were performed by treating the FE simulation results as experimental data [54].

The reliability-based calibrations using both approaches were performed considering the statistical properties of random variables presented in Table 5, with the subscript n denoting nominal properties.

5.1. Eurocode framework

In accordance with Annex D of EN 1990 [68], which specifies the target reliability index for a 50-year reference period, β_{50}, of 3.8, the partial factor, γ_M, required for the NGBoost model was computed with Eq. (1) [71–73,77].

$$\gamma_M = r_n/r_d, \tag{1}$$

where r_n is the nominal resistance predicted by the NGBoost model based on the nominal feature values, and r_d is the design resistance determined from Eq. (2).

$$r_d = b g_{rt}\left(\underline{X}_m\right)\exp\left(-k_{d,\infty}\alpha_{rt}Q_{rt} - k_{d,n}\alpha_\delta Q_\delta - 0.5Q^2\right), \tag{2}$$

where $g_{rt}\left(\underline{X}_m\right)$ is the resistance produced by the NGBoost model using the mean feature values, which were obtained based on the information in Table 5, with all other variables are as defined in EN 1990 [68].

α_{rt}, α_δ, Q_{rt}, and Q in Eq. (2) depend on the CoV, V_{rt}, which was determined from Monte Carlo simulations based on 10,000 sets of random features with the statistical properties from Table 5, similarly to how that was done in [46,78–81]. The reliability analysis was performed for each beam from the database.

Table 6 summarizes the results of the reliability-based calibration of the NGBoost model in accordance with Annex D of EN 1990 [68]. The results indicate that γ_M = 1.00, which is specified in the European design provisions for cellular steel beams [1,23], can be considered appropriate for the developed NGBoost model.

As can be seen from Eqs. (1) and (2), the partial factor depends on the mean ratio of the resistances predicted by the NGBoost model for the nominal and mean feature values, model accuracy (b), and the resistance variability due to the model error (V_δ) and the scatter of the inputs (V_{rt}). Therefore, the differences in the obtained partial factors for different steel grades can be explained as follows.

Table 6
Reliability analysis results for the NGBoost model in accordance with EN 1990 [68] Annex D.

Sreel grade	n	$k_{d,n}$	b	V_δ	V_{rt}	V_r	γ_M
S275	4698	3.04	1.000	0.014	0.056	0.058	0.95
S355	4698	3.04	1.001	0.013	0.088	0.089	1.05
S460	4698	3.04	1.001	0.014	0.001	0.014	1.04
S275, S355, and S460	–	–	–	–	–	–	**1.05**

For all considered steel grades the b and V_δ values were comparable and practically did not contribute to the differences in the γ_M values. On the other hand, the V_{rt} values differed significantly, indicating different levels of the model sensitivity to the variability of the inputs, with the highest scatter produced by the model for steel grade S355 (see Table 6). The beam resistances predicted by the NGBoost model based on the mean values exceeded those based on the nominal values by approximately 26% on average for steel grades S275 and S355, mainly due to the relatively high mean values of f_y/f_{yn} (see Table 5). Therefore, the smaller resistance variability due to the scatter of the inputs (V_{rt}), with all other variables being approximately the same, produced the smaller partial factor for steel grade S275 when compared with steel grade S355. For grade S460 steel, the NGBoost model was practically insensitive to the input scatter and did not show the resistance increase due to the use of the mean input values instead of the nominal input values, resulting in the partial factor approximately equal to that for steel grade S355. It should be noted that partial factors smaller than 1.0 were previously obtained by other researchers [82]. A similar dependence of partial factor values on the steel yield strength was reported in [71,72,82].

5.2. US framework

In the US, cellular steel beams are designed in accordance with AISC DG31 [2], which relies on the AISC 360 [83] provisions. Neither AISC DG31 [2] nor AISC 360 [83] presents a method for evaluating the LRFD resistance factor, ϕ, and the ASD safety factor, Ω, based on experimental data. AISI S100 [69], on the other hand, provides a simple equation for computing the ϕ-factor based on test data (Eq. (3)), which can subsequently be used for obtaining the Ω-factor (Eq. (4)), for cold-formed steel structures.

$$\phi = C_\phi(M_m F_m P_m)e^{-\beta_o\sqrt{V_M^2+V_F^2+C_P V_P^2+V_Q^2}}, \tag{3}$$

where C_ϕ is the calibration coefficient; M_m, F_m, and P_m are mean values of material, fabrication, and professional factors, respectively; V_M, V_F,

Table 7
Reliability analysis results for the NGBoost model in accordance with AISI S100 [69] Chapter K.

Steel grade	n	P_m	V_P	α = 1.0		α = 1.5		α = 2.0	
				ϕ	Ω	ϕ	Ω	ϕ	Ω
S275	4698	1.000	0.014	0.89	1.57	0.88	1.64	0.87	1.69
S355	4698	1.000	0.014	0.89	1.57	0.88	1.64	0.87	1.69
S460	4698	1.000	0.014	0.89	1.57	0.88	1.64	0.87	1.69
S275, S355, and S460	–	–	–	0.89	1.57	0.88	1.64	**0.87**	**1.69**

Table 8
Required resistance reduction factors for the NGBoost model in accordance with the iHL-RF method.

Steel grade	EC framework	US framework	
	γ_M	ϕ	Ω
S275	1.00	1.00	1.43
S355	1.00	1.00	1.45
S460	1.27	0.77	1.91
S275, S355, and S460	**1.09**	**0.92**	**1.60**

and V_P are the CoVs of material, fabrication, and professional factors, respectively; β_o is the target reliability index; $C_P = (1 + 1/n)m/(m - 2)$ is the correction factor; n is the number of samples; $m = n - 1$ are the degrees of freedom; and V_Q is the CoV of load effect.

$$\Omega = (1.2 + 1.6\alpha)/[\phi(1 + \alpha)], \tag{4}$$

where $\alpha = L_n/D_n$, and 1.2 and 1.6 are the LRFD D_n and L_n load factors, respectively, in accordance with ASCE 7 [84].

The reliability-based calibrations of the LRFD methods in accordance with AISC 360 [83] and AISI S100 [69] were based on the same approach [75,85,86] but different live-to-dead load ratios, α: from 1.0 to 2.0 for hot-rolled steel structures [85] and 5.0 for cold-formed steel structures [69]. Therefore, the C_ϕ and V_Q values in Eq. (3) had to be recalculated for α values from 1.0 to 2.0 to apply to hot-rolled steel beams. The method of determining C_ϕ and V_Q based on α, D/D_n, and L/L_n (see Table 5) given in AISI S100 Commentary [69] resulted in C_ϕ = 1.37 and V_Q = 0.13 for α = 1.0, C_ϕ = 1.41 and V_Q = 0.15 for α = 1.5, and C_ϕ = 1.44 and V_Q = 0.17 for α = 2.0.

AISI S100 [69] specifies M_m = 1.10, V_M = 0.10, F_m = 1.00, and V_F = 0.05, which are the same values used in the LRFD method calibration for hot-rolled steel structures [75,85,86]. Therefore, the above values were used in this study. P_m and V_P are the mean and the CoV of RR for the entire dataset (see Table 4). The target reliability index, β_o, was taken as 3.00 according to [75,84,85].

Table 7 summarizes the ϕ- and Ω-factor calculations for different load ratios in accordance with AISI S100 [69]. Table 7 indicates that the most conservative ϕ- and Ω-factors of 0.87 and 1.69, respectively, were obtained for α = 2.0. These values are only slightly more conservative than ϕ = 0.90 and Ω = 1.67 required by AISC DG31 [2] and AISC 360 [83] for cellular steel beams.

5.3. iHL-RF reliability method analyses

In the iHL-RF reliability method [65,66], described in detail in [67], the limit state function is approximated by its first-order Taylor expansion at the design point on the failure boundary. An iterative procedure based on the negative gradient descent with the step size determined using a line search algorithm is employed to find the design point. At each iteration, the Nataf transformation [67,87] is performed to transform correlated random variables into an equivalent space of uncorrelated normally distributed variables, where the reliability index, β, is calculated. This study used the iHL-RF method implemented in a general-purpose package for structural and system reliability analysis, Fortuna.jl [88].

The limit state function was defined by the following equation:

$$G = ME \times R - D - L, \tag{5}$$

where ME is the NGBoost model error; R is the beam resistance; D and L are the applied dead and live loads, respectively.

The NGBoost model error, ME, corresponds to the mean and CoV values of RR for the entire set given in Table 4. Analyses of the RR distributions indicated that they follow lognormal distributions, as Table 5 shows.

The statistical properties of the beam resistance, R, were obtained as follows. As a starting point, 500 random samples of the NGBoost model features were generated following their statistical properties in Table 5. This number of random samples is considered sufficient for obtaining the statistical properties of R [89,90]. The random samples were generated using the Latin Hypercube sampling (LHS) technique [91–94] to ensure that the entire feature ranges and appropriate feature value combinations are represented by the generated random values, which allows for reducing the required number of samples compared with the random sampling. The next step consisted of predicting the ultimate uniform load by the NGBoost model for each set of random features and determining the statistics of R for each analyzed beam. Analyses of the obtained resistance histograms using Fitter (https://fitter.readthedocs.io/en/latest/) indicated that the lognormal distribution is appropriate for R.

The statistical properties of D and L are presented in Table 5. Their nominal values were obtained from Eqs. (6) and (7).

$$D_n = \phi_{RF} R_n/(\gamma_D + \gamma_L \alpha) \tag{6}$$

$$L_n = \alpha \phi_{RF} R_n/(\gamma_D + \gamma_L \alpha). \tag{7}$$

where ϕ_{RF} is the nominal resistance reduction factor, taken as $1/\gamma_M$ for the EC framework, and ϕ and $1/\Omega$ for the US framework's LRFD and ASD methods, respectively; γ_D is the load factor for the dead load (1.35 for the EC framework [68], and 1.2 and 1.0 for the US framework's LRFD and ASD methods, respectively [84]); γ_L is the load factor for the live load (1.5 for the EC framework [68], and 1.6 and 1.0 for the US framework's LRFD and ASD methods, respectively [84]); and $\alpha = L_n/D_n$.

The iHL-RF method reliability analyses were performed for all 14,094 beams from the database [54], considering α values of 0.11, 0.25, 0.50, 1.0, 1.5, and 2.0, with α from 1.0 to 2.0 representing the typical range of the load ratio for hot-rolled steel structures [85]. The obtained reliability indices were compared with target reliability indices of β_{50} = 3.8 [68] for the EC framework and 3.0 [75,84,85] for the US framework.

The reliability analyses were initially carried out assuming ϕ_{RF} = 1.0 for both frameworks. Subsequently, the analyses were repeated with iterated ϕ_{RF} values until the calculated reliability indices for α within 1.0 to 2.0 were equal to or exceeded the target reliability indices. The obtained ϕ_{RF} values were considered the resistance reduction factors required for the NGBoost model to meet the reliability requirements.

Fig. 11 shows the reliability indices determined with the iHL-RF method for ϕ_{RF} = 1.0. It indicates that ϕ = 1.0 is sufficient for the NGBoost model to produce safe predictions only for steel grades S275 and S355 within the EC and US LRFD frameworks.

Table 8 presents values of the resistance reduction factors required for the NGBoost model to meet the reliability requirements for α within 1.0 to 2.0.

It can be seen from this table that the reduction factors become more restrictive when the steel yield strength increases, which can be explained by the higher f_y/f_{yn} values for lower steel grades (see Table 5). In addition, comparisons of the required reduction factors

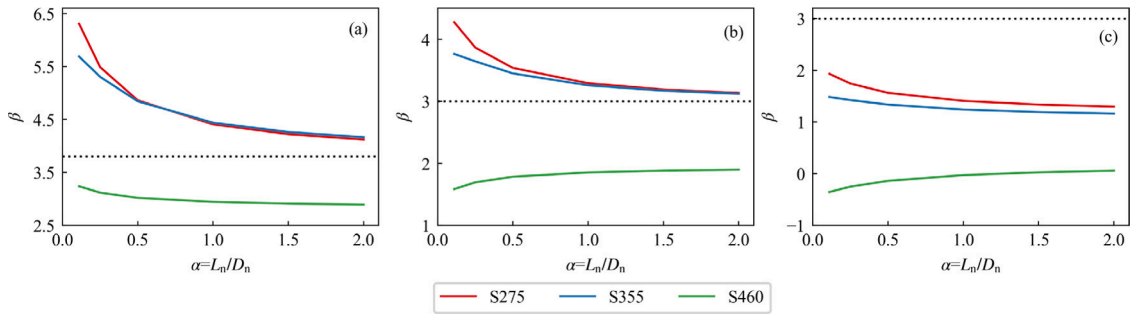

Fig. 11. iHL-RF method analysis results for the resistance predicted by the NGBoost model with no reduction factor (a) EC framework; (b) US framework (LRFD); (c) US framework (ASD).

Table 9
Performance comparison of the NGBoost model with models based on different ML algorithms (nominal resistance).

Model	RMSE (kN/m)			R^2			RR mean			RR CoV		
	Train	Test	All	Train	Test	All	Train	Test	All	Train	Test	All
NGBoost	0.66	1.15	0.79	1.000	0.999	0.999	1.000	1.000	1.000	0.012	0.020	0.014
XGBoost	0.56	1.22	0.74	1.000	0.998	0.999	1.000	1.001	1.000	0.013	0.023	0.016
LightGBM	0.55	1.15	0.71	1.000	0.999	1.000	1.000	1.001	1.000	0.013	0.022	0.015
CatBoost	0.37	1.03	0.57	1.000	0.999	1.000	1.000	0.999	1.000	0.008	0.020	0.012
ANN	0.51	0.92	0.61	1.000	0.999	1.000	1.003	1.003	1.003	0.016	0.026	0.019

from Tables 6, 7, and 8 indicate that the iHL-RF method produced more conservative γ_M values than the EN 1990 [68] Annex D method for all steel grades. For the US framework, the ϕ- and Ω-factors from the iHL-RF method were less restrictive than those obtained from the AISI S100 [69] Chapter K equation.

Based on the reliability analysis results presented in this section, the following resistance reduction factors can be recommended for the NGBoost model: $\gamma_M = 1.09$ for the EC framework (see Table 8), $\phi = 0.87$ for the US LRFD framework, and $\Omega = 1.69$ for the US ASD framework (see Table 7).

6. Comparisons of the NGBoost model performance with other ML models and existing design provisions

Nominal resistance predictions by the NGBoost model were compared with those by other commonly used ML models that previously demonstrated excellent performance on structural engineering problems [29], including XGBoost [57], LightGBM [58], CatBoost [59], and ANN [95] to illustrate the benefits of the proposed model. The XGBoost, LightGBM, CatBoost, and ANN models were trained and optimized with the same methods used for the NGBoost model (see Section 4). Table 9 compares ML model performances on the test, train, and entire subsets. The presented data indicates that all analyzed ML models produced a similar level of accuracy, with the NGBoost model offering probabilistic predictions in addition to deterministic point predictions available in other ML models.

The nominal resistance predictions by the NGBoost model were also compared with those by the existing design provisions, including SCI P355 [1], FprEN 1933-1-13 [23] (with both the main and alternative VBT provisions), and AISC DG31 [2]. The ultimate uniform load determined in accordance with the design provisions based on the governing limit state was treated as the beam resistance. All limit states (failure modes) required by the design provisions were considered in the calculations. The comparison results are presented in Table 10.

It should be noted that the existing design provisions specify different application limits, as follows:

- SCI P355 [1]: $h_o \le 0.8h$ (where $h = H + t_f$); $h_T \ge t_f + 30$ mm (where $h_T = (h - h_o)/2$); $s_o \ge 0.3h_o$; and $s_e \ge 0.5h_o$.
- FprEN 1933-1-13 [23]: $h_o \le 0.8h$; $h_T \ge t_f + 30$ mm; and $s_o \ge 0.1h_o$.
- AISC DG31 [2]: $1.25 \le h/h_o \le 1.75$ and $1.08 \le s/h_o \le 1.5$.

The beams that do not comply with the application limits from the existing design provisions were excluded from the comparisons. As a result, Table 10 shows different numbers of beams, n, for the NGBoost model, which covers the entire database [54], and the design provisions. Table 10 indicates that the proposed NGBoost model significantly outperforms the existing design provisions, which produced relatively high mean and CoV values of the RRs.

Finally, design resistances produced by the NGBoost model and the existing design provisions were compared. In the comparisons, the resistance reduction factors determined in Section 5 ($\gamma_M = 1.09$, $\phi = 0.87$, and $\Omega = 1.69$) were applied to the NGBoost model predictions, and the resistance reduction factors specified in the design provisions ($\gamma_M = 1.00$ for SCI P355 [1] and FprEN 1933-1-13 [23], and $\phi = 0.90$ and $\Omega = 1.67$ for the LRFD and ASD methods of AISC DG31 [2], respectively) were used for their predictions.

The comparison results are presented in Fig. 12 for the EC and US frameworks. Significantly smaller scatters of the NGBoost model predictions than those for the existing design provisions are evident from Fig. 12. It can also be seen that the mean design resistance ratio for the NGBoost model is slightly greater than those for the European design provisions (see Fig. 12(a)). However, a separate study showed that SCI P355 [1] and FprEN 1933-1-13 [23] do not meet the reliability requirements of the Eurocodes [41,68], while the NGBoost model calibration presented in this study ensures its compliance with the reliability requirements. For the US framework, the mean RR values of the NGBoost model are noticeably smaller than those for the LRFD and ASD methods of AISC DG31 [2], demonstrating the economy that can be achieved by using the calibrated NGBoost model.

7. Web application

The developed NGBoost model has been implemented in a web application created in Streamlit (https://streamlit.io). The web application is available at https://scbra.herokuapp.com/. It allows for rapid probabilistic predictions of the load-bearing capacities for laterally restrained cellular steel beams subject to uniformly distributed loads based on the feature values selected by the user. Only the feature values within the model applicability limits are available for the selections to ensure that the model is not used outside its scope corresponding to the variable ranges in the database [54] used for the model training (see Table 2). The web application applies to both the EC and US design frameworks.

Table 10
Performance comparison of the NGBoost model with the existing design provisions (nominal resistance).

Model	n	RMSE (kN/m)	R^2	RR min.	RR max.	RR mean	RR CoV
NGBoost	14 094	0.79	0.999	0.83	1.09	1.00	0.014
SCI P355 [1]	2997	29.43	−0.037	0.88	16.57	1.66	0.647
Fpr EN 1993-1-13[a] [23]	13 554	21.06	0.551	0.70	16.62	1.37	0.676
Fpr EN 1993-1-13[b] [23]	13 554	22.92	0.468	0.70	21.99	1.49	0.911
AISC DG31 [2]	10 854	21.69	0.506	0.85	2.77	1.58	0.181

Notes:
[a] Main provisions for the Vierendeel bending of the Tees.
[b] Alternative provisions for the Vierendeel bending of the Tees.

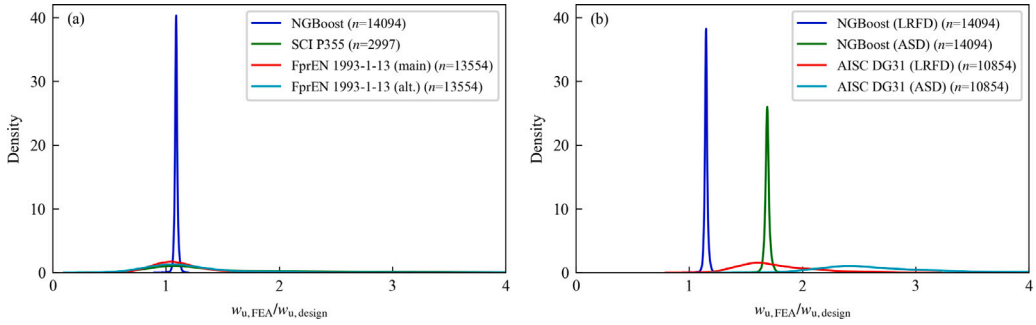

Fig. 12. Distributions of the design resistance ratios computed with the NGBoost model and existing design provisions (a) EC framework; (b) US framework.

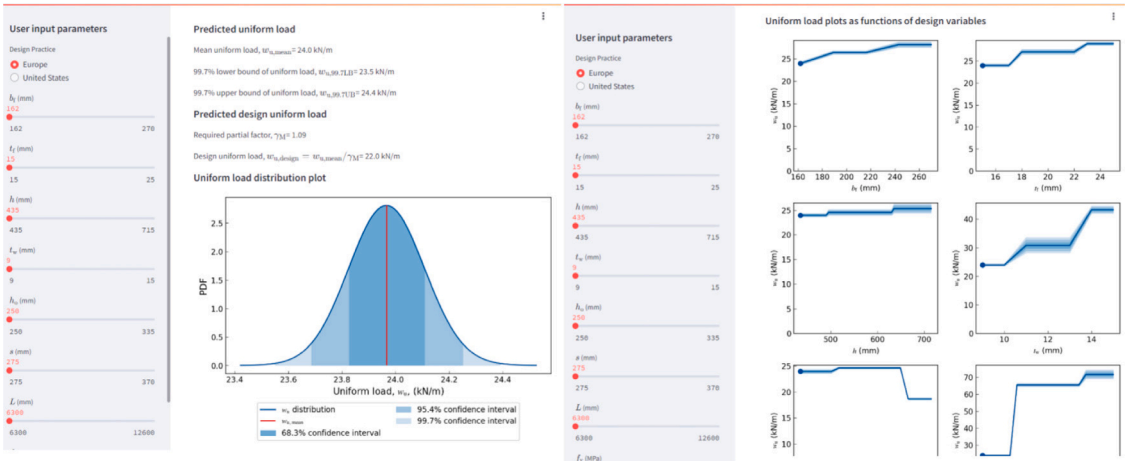

Fig. 13. GUI interface of the web application.

In the web application, probabilistic point predictions are supplemented with interactive plots of the ultimate uniform loads as functions of the model features, showing probabilistic confidence intervals determined by the NGBoost model. The web application's graphical user interface (GUI) is shown in Fig. 13.

8. Conclusions

This paper proposes an NGBoost model for probabilistic predictions of the ultimate uniform loads of laterally restrained cellular steel beams. The model was developed using a database of 14,094 numerical results from FE models validated against test data. The database covers cellular steel beams with various parameter values representing those used in construction.

The proposed NGBoost model was optimized by fine-tuning its hyperparameters for improved prediction accuracy and overfitting minimization. The NGBoost model was interpreted with the SHAP method, which showed that the beam span and the web opening spacing have the most significant effects on the ultimate loads predicted by the model. Steel yield strength, web thickness, beam height, flange thickness and width, and web opening diameter affect the predicted ultimate loads less significantly than the span length and web opening spacing. The parity of the number of web openings (odd or even) was the least influential parameter.

The NGBoost model was calibrated for the EC and US design frameworks via reliability analyses in accordance with the respective design standards, as well as by using the improved Hasofer–Lind–Rackwitz–Fiessler (iHL-RF) method. The resistance reduction factors required for the NGBoost model to meet the reliability requirements of the respective European and US design standards were determined from the reliability analyses.

Comparisons of the predictions by the NGBoost model with those by the XGBoost, LightGBM, CatBoost, and ANN models and the existing design provisions indicate that the NGBoost model is as accurate as the other analyzed ML models while offering probabilistic predictions unavailable in other analyzed ML models. The NGBoost model significantly outperforms the existing design provisions, including SCI P355 [1], FprEN 1993-1-13 [23], and AISC DG31 [2].

It should be noted that the probabilistic model does not offer significant benefits over the deterministic ML models for practical design, which uses deterministic resistance values. However, the probabilistic

predictions may help the designer better understand the predicted resistance variability and make informed decisions about the available margins of safety. The probabilistic predictions also provide insights into the beam parameters producing high resistance variability, helping to identify potential opportunities for design optimization.

An NGBoost model-based web application for predicting the nominal and design values of the ultimate uniform load of laterally restrained cellular steel beams was developed and published online. In addition to probabilistic point predictions, the web application produces plots of the ultimate loads as functions of the input parameters with probabilistic confidence intervals, contributing to the model's explainability and interpretability.

The proposed reliability-based calibrated NGBoost model can be used to select beam sizes in preliminary designs and investigate the beam parameters affecting their resistance. The probabilistic NGBoost model predictions allow for evaluating expected resistance ranges and selecting the resistance based on a desired confidence interval.

CRediT authorship contribution statement

Vitaliy V. Degtyarev: Writing – original draft, Visualization, Validation, Software, Methodology, Investigation, Formal analysis, Data curation. **Stephen J. Hicks:** Writing – review & editing, Validation, Supervision, Methodology, Investigation, Conceptualization. **Felipe Piana Vendramell Ferreira:** Writing – review & editing, Validation, Supervision, Investigation, Conceptualization. **Konstantinos Daniel Tsavdaridis:** Writing – review & editing, Validation, Supervision, Project administration, Methodology, Investigation, Conceptualization.

Declaration of competing interest

The authors declare that they have no known competing financial interests or personal relationships that could have appeared to influence the work reported in this paper.

Data availability

The database used in the study has been made publicly available (https://data.mendeley.com/datasets/zcm29bp7yf/1) and is referenced in the manuscript. The developed web application can be accessed at https://scbra.herokuapp.com/.

Acknowledgments

The authors wish to extend their thanks to Damir Akchurin, a Ph.D. student at Johns Hopkins University, for developing the Fortuna package and its public accessibility, as well as for his indispensable support in its application.

References

[1] R. Lawson, S. Hicks, Design of Composite Beams with Large Web Openings SCI P355, Steel Construction Institute, Berkshire, UK, 2011.
[2] S. Fares, J. Coulson, D. Dinehart, Design Guide 31: Castellated and Cellular Beam Design, American Institute of Steel Construction, Chicago, IL, USA, 2016.
[3] J. Warren, Ultimate Load and Deflection Behaviour of Cellular Beams (Master's thesis), University of Natal, Durban, South Africa, 2001.
[4] C. Müller, O. Hechler, A. Bureau, D. Bitar, D. Joyeux, L. Cajot, T. Demarco, R. Lawson, S. Hicks, P. Devine, O. Lagerqvist, E. Hedman-Pétursson, E. Unosson, M. Feldmann, Large Web Openings for Service Integration in Composite Floors, Report EUR 21345, European Commission, Brussels, Belgium, 2006.
[5] K.D. Tsavdaridis, C. D'Mello, Web buckling study of the behaviour and strength of perforated steel beams with different novel web opening shapes, J. Constr. Steel Res. 67 (10) (2011) 1605–1620, http://dx.doi.org/10.1016/j.jcsr.2011.04.004.
[6] F. Erdal, M.P. Saka, Ultimate load carrying capacity of optimally designed steel cellular beams, J. Constr. Steel Res. 80 (2013) 355–368, http://dx.doi.org/10.1016/j.jcsr.2012.10.007.
[7] D. Sonck, Global Buckling of Castellated and Cellular Steel Beams and Columns (Ph.D. thesis), Ghent University, Ghent, Belgium, 2014.
[8] S.G. Morkhade, L.M. Gupta, An experimental and parametric study on steel beams with web openings, Int. J. Adv. Struct. Eng. (IJASE) 7 (3) (2015) 249–260, http://dx.doi.org/10.1007/s40091-015-0095-4.
[9] L.F. Grilo, R.H. Fakury, A.L.R. de Castro e Silva, G.d. Veríssimo, Design procedure for the web-post buckling of steel cellular beams, J. Constr. Steel Res. 148 (2018) 525–541, http://dx.doi.org/10.1016/j.jcsr.2018.06.020.
[10] L. Kang, S. Hong, X. Liu, Shear behaviour and strength design of cellular beams with circular or elongated openings, Thin-Walled Struct. 160 (2021) 107353, http://dx.doi.org/10.1016/j.tws.2020.107353.
[11] J. Nseir, M. Lo, D. Sonck, H. Somja, O. Vassart, N. Boissonnade, Lateral torsional buckling of cellular steel beams, in: Structural Stability Research Council Annual Stability Conference (SSRC2012), Grapevine, TX, USA, 2012.
[12] K. Rajana, K.D. Tsavdaridis, E. Koltsakis, Elastic and inelastic buckling of steel cellular beams under strong-axis bending, Thin-Walled Struct. 156 (2020) 106955, http://dx.doi.org/10.1016/j.tws.2020.106955.
[13] A. Jamadar, P. Kumbhar, Parametric study of castellated beam with circular and diamond shaped openings, Int. Res. J. Eng. Technol. 2 (2) (2015) 715–722, http://dx.doi.org/10.1016/j.tws.2020.106955.
[14] A.M. Sweedan, Elastic lateral stability of I-shaped cellular steel beams, J. Constr. Steel Res. 67 (2) (2011) 151–163, http://dx.doi.org/10.1016/j.jcsr.2010.08.009.
[15] M.I.M.H. Martini, Elasto-Plastic Lateral Torsional Buckling of Steel Beams with Perforated Web (Ph.D. thesis), United Arab Emirates University, 2011.
[16] D. Sonck, J. Belis, Lateral–torsional buckling resistance of cellular beams, J. Constr. Steel Res. 105 (2015) 119–128, http://dx.doi.org/10.1016/j.jcsr.2014.11.003.
[17] P. Panedpojaman, W. Sae-Long, T. Chub-uppakarn, Cellular beam design for resistance to inelastic lateral–torsional buckling, Thin-Walled Struct. 99 (2016) 182–194, http://dx.doi.org/10.1016/j.tws.2015.08.026.
[18] F.P.V. Ferreira, A. Rossi, C.H. Martins, Lateral-torsional buckling of cellular beams according to the possible updating of EC3, J. Constr. Steel Res. 153 (2019) 222–242, http://dx.doi.org/10.1016/j.jcsr.2018.10.011.
[19] P. Panedpojaman, T. Thepchatri, S. Limkatanyu, Novel design equations for shear strength of local web-post buckling in cellular beams, Thin-Walled Struct. 76 (2014) 92–104, http://dx.doi.org/10.1016/j.tws.2013.11.007.
[20] E. Ellobody, Nonlinear analysis of cellular steel beams under combined buckling modes, Thin-Walled Struct. 52 (2012) 66–79, http://dx.doi.org/10.1016/j.tws.2011.12.009.
[21] J. Ward, Design of Composite and Non-Composite Cellular Beams SCI P100, Steel Construction Institute, Berkshire, UK, 1990.
[22] ENV 1993-1-1: 1992/A2: 1998, Eurocode 3: Design of Steel Structures — Part 1-1: General Rules — General Rules and Rules for Buildings - Amendment A2, European Committee for Standardization, Brussels, Belgium, 1998.
[23] FprEN 1993-1-13, Eurocode 3: Design of steel structures - Part 1-13: Rules for beams with large web openings, European Committee for Standardization, Brussels, Belgium, 2023.
[24] P. Panedpojaman, W. Sae-Long, Accuracy of available methods to evaluate Vierendeel failure load, in: Transactions on Engineering Technologies: World Congress on Engineering 2014, Springer, 2015, pp. 163–175, http://dx.doi.org/10.1007/978-94-017-9804-4_11.
[25] V. Akrami, S. Erfani, Review and assessment of design methodologies for perforated steel beams, J. Struct. Eng. 142 (2) (2016) 04015148, http://dx.doi.org/10.1061/(ASCE)ST.1943-541X.0001421.
[26] F.P.V. Ferreira, C.H. Martins, LRFD for lateral-torsional buckling resistance of cellular beams, Int. J. Civ. Eng. 18 (3) (2020) 303–323, http://dx.doi.org/10.1007/s40999-019-00474-7.
[27] H. Salehi, R. Burgueño, Emerging artificial intelligence methods in structural engineering, Eng. Struct. 171 (2018) 170–189, http://dx.doi.org/10.1016/j.engstruct.2018.05.084.
[28] H. Sun, H.V. Burton, H. Huang, Machine learning applications for building structural design and performance assessment: State-of-the-art review, J. Build. Eng. 33 (2021) 101816, http://dx.doi.org/10.1016/j.jobe.2020.101816.
[29] H.-T. Thai, Machine learning for structural engineering: A state-of-the-art review, Structures 38 (2022) 448–491, http://dx.doi.org/10.1016/j.istruc.2022.02.003.
[30] Y. Sharifi, A. Moghbeli, M. Hosseinpour, H. Sharifi, Neural networks for lateral torsional buckling strength assessment of cellular steel I-beams, Adv. Struct. Eng. 22 (9) (2019) 2192–2202, http://dx.doi.org/10.1177/1369433219836176.
[31] M. Abambres, K. Rajana, K.D. Tsavdaridis, T.P. Ribeiro, Neural network-based formula for the buckling load prediction of I-section cellular steel beams, Computers 8 (1) (2019) 2, http://dx.doi.org/10.3390/computers8010002.
[32] H.-B. Ly, T.-T. Le, L.M. Le, V.Q. Tran, V.M. Le, H.-L.T. Vu, Q.H. Nguyen, B.T. Pham, Development of hybrid machine learning models for predicting the critical buckling load of I-shaped cellular beams, Appl. Sci. 9 (24) (2019) 5458, http://dx.doi.org/10.3390/app9245458.
[33] V. Limbachiya, R. Shamass, Application of artificial neural networks for web-post shear resistance of cellular steel beams, Thin-Walled Struct. 161 (2021) 107414, http://dx.doi.org/10.1016/j.tws.2020.107414.
[34] F.P.V. Ferreira, R. Shamass, V. Limbachiya, K.D. Tsavdaridis, C.H. Martins, Lateral–torsional buckling resistance prediction model for steel cellular beams generated by Artificial Neural Networks (ANN), Thin-Walled Struct. 170 (2022) 108592, http://dx.doi.org/10.1016/j.tws.2021.108592.

[35] V.V. Degtyarev, K.D. Tsavdaridis, Buckling and ultimate load prediction models for perforated steel beams using machine learning algorithms, J. Build. Eng. (ISSN: 2352-7102) 51 (2022) 104316, http://dx.doi.org/10.1016/j.jobe.2022.104316.

[36] M.E.A.B. Seghier, H. Carvalho, C.C. de Faria, J.A. Correia, R.H. Fakury, Numerical analysis and prediction of lateral-torsional buckling resistance of cellular steel beams using FEM and least square support vector machine optimized by metaheuristic algorithms, Alexandria Eng. J. 67 (2023) 489–502, http://dx.doi.org/10.1016/j.aej.2022.12.062.

[37] M. Hosseinpour, Y. Sharifi, H. Sharifi, Neural network application for distortional buckling capacity assessment of castellated steel beams, in: Structures, Vol. 27, Elsevier, 2020, pp. 1174–1183, http://dx.doi.org/10.1016/j.istruc.2020.07.027.

[38] R. Shamass, F.P.V. Ferreira, V. Limbachiya, L.F.P. Santos, K.D. Tsavdaridis, Web-post buckling prediction resistance of steel beams with elliptically-based web openings using Artificial Neural Networks (ANN), Thin-Walled Struct. 180 (2022) 109959, http://dx.doi.org/10.1016/j.tws.2022.109959.

[39] M. Rabi, Y.S. Jweihan, I. Abarkan, F.P.V. Ferreira, R. Shamass, V. Limbachiya, K.D. Tsavdaridis, L.F.P. Santos, Machine learning-driven web-post buckling resistance prediction for high-strength steel beams with elliptically-based web openings, Results Eng. 21 (2024) 101749, http://dx.doi.org/10.1016/j.rineng.2024.101749.

[40] A.S. de Carvalho, M. Hosseinpour, A. Rossi, C.H. Martins, Y. Sharifi, New formulas for predicting the lateral–torsional buckling strength of steel I-beams with sinusoidal web openings, Thin-Walled Struct. 181 (2022) 110067, http://dx.doi.org/10.1016/j.tws.2022.110067.

[41] EN 1993-1-1, Eurocode 3 - Design of Steel Structures - Part 1-1: General Rules and Rules for Buildings, European Committee for Standardization, Brussels, Belgium, 2022.

[42] S. Hicks, R. Lawson, J. Rackham, P. Fordham, Comparative Structure Cost of Modern Commercial Buildings (Second Edition) SCI P137, Steel Construction Institute, Berkshire, UK, 2004.

[43] T. Duan, A. Anand, D.Y. Ding, K.K. Thai, S. Basu, A. Ng, A. Schuler, Ngboost: Natural gradient boosting for probabilistic prediction, in: 37th International Conference on Machine Learning, PMLR, 2020, pp. 2690–2700.

[44] S.-Z. Chen, D.-C. Feng, W.-J. Wang, E. Taciroglu, Probabilistic machine-learning methods for performance prediction of structure and infrastructures through natural gradient boosting, J. Struct. Eng. 148 (8) (2022) 04022096, http://dx.doi.org/10.1061/(ASCE)ST.1943-541X.0003401.

[45] Y. Mei, Y. Sun, F. Li, X. Xu, A. Zhang, J. Shen, Probabilistic prediction model of steel to concrete bond failure under high temperature by machine learning, Eng. Fail. Anal. 142 (2022) 106786, http://dx.doi.org/10.1016/j.engfailanal.2022.106786.

[46] V.V. Degtyarev, S.J. Hicks, Machine learning-based probabilistic predictions of shear resistance of welded studs in deck slab ribs transverse to beams, Steel Compos. Struct. 49 (1) (2023) 109–123, http://dx.doi.org/10.12989/scs.2023.49.1.109.

[47] P.C. Lazaridis, I.E. Kavvadias, K. Demertzis, L. Iliadis, L.K. Vasiliadis, Interpretable machine learning for assessing the cumulative damage of a reinforced concrete frame induced by seismic sequences, Sustainability 15 (17) (2023) 12768, http://dx.doi.org/10.3390/su151712768.

[48] M.-Y. Liu, Z. Li, H. Zhang, Probabilistic shear strength prediction for deep beams based on Bayesian-optimized data-driven approach, Buildings 13 (10) (2023) 2471, http://dx.doi.org/10.3390/buildings13102471.

[49] S. Liang, Y. Cai, Z. Fei, Y. Shen, Multi-objective optimization design of FRP reinforced flat slabs under punching shear by using NGBoost-Based Surrogate Model, Buildings 13 (11) (2023) 2727, http://dx.doi.org/10.3390/buildings13112727.

[50] V.-L. Tran, D.-K. Thai, J.-K. Kim, Machine learning-based model for moment capacity prediction and reliability analysis of PSC beams, Structures 62 (2024) 106181, http://dx.doi.org/10.1016/j.istruc.2024.106181.

[51] D. Sonck, R. Van Impe, J. Belis, Experimental investigation of residual stresses in steel cellular and castellated members, Constr. Build. Mater. 54 (2014) 512–519, http://dx.doi.org/10.1016/j.conbuildmat.2013.12.045.

[52] prEN 1993-1-14, Eurocode 3: Design of Steel Structures - Part 1-14: Design Assisted by Finite Element Analysis, European Committee for Standardization, Brussels, Belgium, 2023.

[53] EN 10025-2, Hot Rolled Products of Structural Steels - Part 2: Technical Delivery Conditions for Non-Alloy Structural Steels, European Committee for Standardization, Brussels, Belgium, 2019.

[54] V.V. Degtyarev, S.J. Hicks, F.P.V. Ferreira, K.D. Tsavdaridis, Database of the Uniform Ultimate Loads Applied to Laterally Restrained Cellular Steel Beams, V.1, Mendeley Data, 2024, http://dx.doi.org/10.17632/zcm29bp7yf.1.

[55] J.H. Friedman, Greedy function approximation: a gradient boosting machine, Ann. Statist. 29 (5) (2001) 1189–1232, http://dx.doi.org/10.1214/aos/1013203451.

[56] S.-I. Amari, Natural gradient works efficiently in learning, Neural Comput. 10 (2) (1998) 251–276, http://dx.doi.org/10.1162/089976698300017746.

[57] T. Chen, C. Guestrin, XGBoost: A scalable tree boosting system, in: Proceedings of the 22nd ACM SIGKDD International Conference on Knowledge Discovery and Data Mining, 2016, pp. 785–794, http://dx.doi.org/10.1145/2939672.2939785.

[58] G. Ke, Q. Meng, T. Finley, T. Wang, W. Chen, W. Ma, Q. Ye, T.-Y. Liu, LightGBM: A highly efficient gradient boosting decision tree, Adv. Neural Inf. Process. Syst. 30 (2017) 3146–3154.

[59] A.V. Dorogush, V. Ershov, A. Gulin, CatBoost: gradient boosting with categorical features support, 2018, http://dx.doi.org/10.48550/arXiv.1810.11363, arXiv preprint arXiv:1810.11363.

[60] F. Pedregosa, G. Varoquaux, A. Gramfort, V. Michel, B. Thirion, O. Grisel, et al., Scikit-learn: Machine learning in Python, J. Mach. Learn. Res. 12 (2011) 2825–2830.

[61] D. Chicco, M.J. Warrens, G. Jurman, The coefficient of determination R-squared is more informative than SMAPE, MAE, MAPE, MSE and RMSE in regression analysis evaluation, PeerJ Comput. Sci. 7 (2021) e623.

[62] T. Akiba, S. Sano, T. Yanase, T. Ohta, M. Koyama, Optuna: A next-generation hyperparameter optimization framework, in: Proceedings of the 25th ACM SIGKDD International Conference on Knowledge Discovery & Data Mining, 2019, pp. 2623–2631, http://dx.doi.org/10.1145/3292500.3330701.

[63] S. Lundberg, S.-I. Lee, A unified approach to interpreting model predictions, 2017, http://dx.doi.org/10.48550/arXiv.1705.07874, arXiv preprint arXiv:1705.07874.

[64] B. Peleg, P. Sudhölter, Introduction to the Theory of Cooperative Games, Springer Science & Business Media, 2007.

[65] A.M. Hasofer, N.C. Lind, Exact and invariant second-moment code format, J. Eng. Mech. Div. 100 (1) (1974) 111–121, http://dx.doi.org/10.1061/JMCEA3.000184.

[66] R. Rackwitz, B. Flessler, Structural reliability under combined random load sequences, Comput. Struct. 9 (5) (1978) 489–494, http://dx.doi.org/10.1016/0045-7949(78)90046-9.

[67] A. Der Kiureghian, Structural and System Reliability, Cambridge University Press, 2022.

[68] EN 1990:2002+A1, Eurocode: Basis of Structural Design, European Committee for Standardization, Brussels, Belgium, 2005.

[69] ANSI/AISI S100-16 (R2020) w/S3-22, North American Specification for the Design of Cold-Formed Steel Structural Members, American Institute of Steel Construction, Chicago, Illinois, USA, 2022.

[70] J. Gomes Jr., H. Carvalho, L.S. da Silva, J. Ferreira Filho, A. Lavall, Assessment of design procedures for the buckling resistance of hot-rolled steel equal leg angles under concentric and eccentric compression, Structures 57 (2023) 105308, http://dx.doi.org/10.1016/j.istruc.2023.105308.

[71] X. Meng, L. Gardner, Testing, modelling and design of normal and high strength steel tubular beam-columns, J. Constr. Steel Res. 183 (2021) 106735, http://dx.doi.org/10.1016/j.jcsr.2021.106735.

[72] B. Behzadi-Sofiani, L. Gardner, M.A. Wadee, Behaviour, finite element modelling and design of cruciform section steel columns, Thin-Walled Struct. 182 (2023) 110124, http://dx.doi.org/10.1016/j.tws.2022.110124.

[73] X. Yun, Y. Zhu, X. Meng, L. Gardner, Welded steel I-section columns: residual stresses, testing, simulation and design, Eng. Struct. 282 (2023) 115631, http://dx.doi.org/10.1016/j.engstruct.2023.115631.

[74] EN 1090-2, Execution of Steel Structures and Aluminium Structures - Part 2: Technical Requirements for Steel Structures, European Committee for Standardization, Brussels, Belgium, 2018.

[75] T.V. Galambos, Load and resistance factor design, AISC Eng. J. 18 (3) (1981) 74–82.

[76] H. Gulvanessian, M. Holicky, Eurocodes: using reliability analysis to combine action effects, Proc. Inst. Civ. Eng.-Struct. Build. 158 (4) (2005) 243–252, http://dx.doi.org/10.1680/stbu.2005.158.4.243.

[77] S. Afshan, P. Francis, N. Baddoo, L. Gardner, Reliability analysis of structural stainless steel design provisions, J. Constr. Steel Res. 114 (2015) 293–304, http://dx.doi.org/10.1016/j.jcsr.2015.08.012.

[78] S.J. Hicks, Design shear resistance of headed studs embedded in solid slabs and encasements, J. Constr. Steel Res. 139 (2017) 339–352, http://dx.doi.org/10.1016/j.jcsr.2017.09.018.

[79] V.V. Degtyarev, S.J. Hicks, J.F. Hajjar, Design models for predicting shear resistance of studs in solid concrete slabs based on symbolic regression with genetic programming, Steel Compos. Struct. 43 (3) (2022) 293–309, http://dx.doi.org/10.12989/scs.2022.43.3.293.

[80] V.V. Degtyarev, S.J. Hicks, Reliability-based design shear resistance of headed studs in solid slabs predicted by machine learning models, Archit. Struct. Constr. (2022) 1–27, http://dx.doi.org/10.1007/s44150-022-00078-1.

[81] V.V. Degtyarev, S.J. Hicks, Shear resistance of welded studs in deck slab ribs transverse to beams, Eng. Struct. 294 (2023) 116709, http://dx.doi.org/10.1016/j.engstruct.2023.116709.

[82] J. Spiegler, L. Simões da Silva, O. Vassart, L. Marques, N. Popa, L. Cajot, et al., Standardization of Safety Assessment Procedures Across Brittle to Ductile Failure Modes (SAFEBRICTILE) : Final Report, Publications Office of the European Union, Luxembourg, 2018, http://dx.doi.org/10.2777/76892.

[83] ANSI/AISC 360-22, Specification for Structural Steel Buildings, American Institute of Steel Construction, Chicago, Illinois, USA, 2022.

[84] ASCE/SEI 7-22, Minimum Design Loads and Associated Criteria for Buildings and Other Structures, American Society of Civil Engineers, Reston, VA, USA, 2022.

[85] B. Ellingwood, B. Galambos, J. MacGregor, C. Cornell, Development of a Probability Based Load Criterion for American National Standard A58: Building Code Requirements for Minimum Design Loads in Buildings and Other Structures, vol. 577, Department of Commerce, National Bureau of Standards, 1980.
[86] M. Ravindra, T. Galambos, Load and resistance factor design for steel, J. Struct. Div. 104 (9) (1978) 1337–1353, http://dx.doi.org/10.1061/JSDEAG.0004981.
[87] A. Nataf, Détermination des distribution dont les marges sont données, C. R. l'Acad. Sci. 225 (1962) 42–43.
[88] D. Akchurin, Fortuna.jl: Structural and system reliability analysis in Julia, J. Open Source Softw. 9 (100) (2024) 6967, http://dx.doi.org/10.21105/joss.06967.
[89] R.E. Melchers, A.T. Beck, Structural Reliability Analysis and Prediction, John Wiley & Sons, 2018.
[90] V.V. Degtyarev, H.-T. Thai, Design of concrete-filled steel tubular columns using data-driven methods, J. Constr. Steel Res. 200 (2023) 107653, http://dx.doi.org/10.1016/j.jcsr.2022.107653.
[91] M.D. McKay, R.J. Beckman, W.J. Conover, A comparison of three methods for selecting values of input variables in the analysis of output from a computer code, Technometrics 42 (1) (2000) 55–61, http://dx.doi.org/10.2307/1268522.
[92] V. Eglajs, P. Audze, New approach to the design of multifactor experiments, Probl. Dyn. Strengths 35 (1) (1977) 104–107.
[93] R.L. Iman, J.C. Helton, J.E. Campbell, An approach to sensitivity analysis of computer models: Part I—Introduction, input variable selection and preliminary variable assessment, J. Qual. Technol. 13 (3) (1981) 174–183, http://dx.doi.org/10.1080/00224065.1981.11978748.
[94] R.L. Iman, J.M. Davenport, D.K. Zeigler, Latin Hypercube Sampling (Program User's Guide).[LHC, in FORTRAN], Tech. Rep., Sandia Labs., Albuquerque, NM (USA), 1980.
[95] C.C. Aggarwal, Neural Networks and Deep Learning: A Textbook, Springer, 2018.